Polarization of 220-Mev Protons Elastically Scattered from Carbon*

W. G. CHESNUT,† E. M. HAFNER, AND A. ROBERTS
University of Rochester, Rochester, New York

(Received July 9, 1956)

Protons polarized to 89% have been scattered from C^{12} in the laboratory angular range from 4 to 40 degrees. Data were obtained on angular distributions and asymmetries in three closely spaced energy channels spanning the high-energy tail of the incident spectrum. In spite of the great width of this spectrum, it was possible to extrapolate the data so as to give fair separation of elastic from inelastic scattering. The elastic asymmetries exhibit clear evidence of a deep minimum at 27 degrees followed by a strong maximum at 35 degrees, in qualitative agreement with various predictions from $L\cdot S$ coupling in an optical model of the scattering. Possible reasons are given for the failure of the minimum to appear in the results of other experimenters.

I. INTRODUCTION

SOON after the discovery by Oxley *et al.*[1] that large polarizations are produced in the scattering of high-energy protons from nuclei, Dickson and Salter[2] found evidence that double-scattering asymmetries involving inelastic processes may be quite different from those observed in elastic scattering. With these results at hand, we began an investigation of polarization in the elastic scattering of 220-Mev protons from various complex nuclei. Our first effort was directed toward an understanding of the scattering from C^{12}, since the information would be of assistance in the investigation of proton-proton polarization by means of a CH_2-C difference method. In addition, the results would be used to calibrate the polarization of beams produced by scattering from a first target of C^{12}.

Very early in the investigation we learned that, at scattering angles above about 15°, the experimental asymmetries are extremely sensitive to the energy threshold (and thus to the inelastic contribution) in the detecting telescope, even when attention is confined to very few of the lowest energy states of C^{12}. After some thought, we decided to pursue the study of this nucleus in an attempt to improve the discrimination against inelastic scattering. The first excited state of C^{12} is 4.43 Mev above the ground state, and we assumed that the separation would be sufficiently large to make the discrimination possible without great difficulty. The results presented here show that this assumption was not entirely justified, in view of the fact that there are angular regions in which the inelastic scattering from C^{12} is ten or more times as intense as the elastic scattering. We felt, however, that the significance of the measurements would depend greatly on the success of the energy discrimination, particularly if we wished to make quantitative comparison with the several theoretical descriptions[3–7] that were beginning to appear. We could, of course, also expect to derive information about the inelastic scattering, for which there is as yet no theoretical treatment.

The ideal solution to the problem of energy discrimination would follow from the production of a highly monoenergetic polarized proton beam, which might then be separated after scattering into groups corresponding to different final states of the second target. Our attempts to accomplish this have so far been disappointing: the spread in cyclotron beam energy is quite large, and the beam intensity in a suitably narrow energy interval is too low for reasonable counting rates at large scattering angles. Alternative procedures had to be considered. The method finally used is an extrapolation procedure that enables us to estimate purely elastic effects with reasonable accuracy, despite an incident energy spread of 15 to 20 Mev. We suggest that this approach might be useful in other experiments, e.g., in high-energy neutron scattering, where the production of a monoenergetic neutron beam is extremely difficult. In the light of certain developments[8] in synchrocyclotron operation, it may now be possible to obtain a monoenergetic polarized beam by employing a regenerator[9] and a first scatterer at large radius.[10] This procedure has not yet been investigated, and the present report is confined to a description of the extrapolation method and of the results obtained up to the present.

II. EXPERIMENTAL PROCEDURE

Figure 1 is a schematic diagram of the 130-inch cyclotron, including the essentials of the double-scattering equipment used in the present measurements. The circulating proton beam strikes an internal graphite target. Protons that scatter at approximately

* Research supported by the U. S. Atomic Energy Commission.

† Now at Brookhaven National Laboratory, Upton, New York. This report constitutes a part of Dr. Chesnut's Ph.D. thesis.

[1] Oxley, Cartwright, and Rouvina, Phys. Rev. **93**, 806 (1954).

[2] J. M. Dickson and D. C. Salter, Nature **173**, 946 (1954).

[3] E. Fermi, Nuovo cimento **11**, 407 (1954).

[4] Snow, Sternheimer, and Yang, Phys. Rev. **94**, 1073 (1954).

[5] B. J. Malenka, Phys. Rev. **95**, 522 (1954).

[6] R. M. Sternheimer, Phys. Rev. **95**, 587 (1954).

[7] W. Heckrotte and J. V. Lepore, Phys. Rev. **95**, 1109 (1954).

[8] A. V. Crewe and J. W. G. Gregory, Proc. Roy. Soc. (London) **A232**, 242 (1955).

[9] K. J. LeCouteur and S. Lipton, Phil. Mag. **46**, 1265 (1955).

[10] We are indebted to Dr. Richard Wilson for this suggestion.

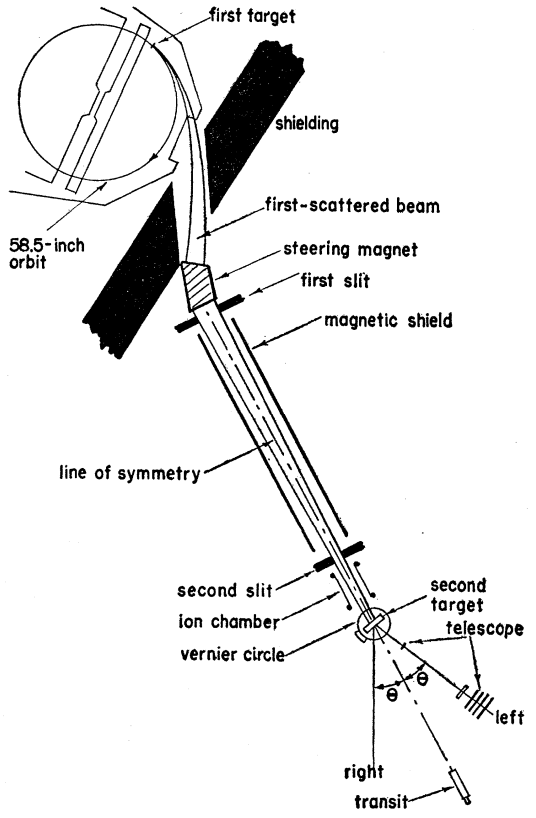

FIG. 1. Schematic diagram of double-scattering equipment. Both targets are made of graphite. The angle of first scattering is 14.0 degrees, and the polarization of the first-scattered proton beam has been found to be 89%.

14° are collected and focused by a steering magnet, and subsequently defined by two slits about 10 feet apart. The region between the slits is magnetically shielded from the cyclotron fringing field. The second slit limits the area of second scatterer exposed to the beam, which is monitored by an air-filled ionization chamber. After second scattering, protons pass through a six-counter telescope containing copper absorbers for selection of appropriate energy intervals. The relative rates observed in successive counters are determined by three factors: (i) the spectrum of the incident (first-scattered) beam; (ii) the relative amounts of scattering corresponding to the possible energy states of the target nucleus; and (iii) losses caused by inefficiency, absorption, and multiple scattering in the counters. When the telescope is in the direct beam, or when it is set at a small enough angle so that elastic scattering predominates, the first and third factors combine to give what can be called an "incident" spectrum. At larger angles, where inelastic scattering becomes significant, the ratios of successive counter yields are altered in a way that reflects changes in the scattered spectrum. In principle, then, it is possible to use the *deviations* of these ratios from the incident spectrum in order to deduce the relative contributions of elastic and inelastic scattering. We wish here to describe two possible ways of handling the problem, and to deal very briefly with the most significant features of the experimental problems.

A. Separation Techniques

In order to illustrate the extrapolation method, let us assume that we have a five-counter telescope consisting of thin scintillators separated by absorbers so chosen that the energy loss between successive counters is equal to the separation of the ground and first excited states of the target nucleus. The counters are numbered from 1 to 5 in the order in which they are seen by the scattered beam. A thick absorber is placed ahead of counter 1, and is adjusted until the telescope sees only those protons that originate in the high-energy tail of the incident spectrum. We define as "channels" the energy intervals of the incident beam that lead to *elastic* scattering into the various counters. For instance, "channel 4" covers all energies above the lowest that scatters elastically into counter 4; "channel 4–5" is the interval that scatters elastically into counter 4 but not into counter 5. It is now clear that, as a result of our choice of channels, *inelastic* scattering leaving the target nucleus in its first excited state involves a shift downward by one channel. We must also, of course, consider the possibility of inelastic scattering in which higher states are excited. It is known[11] that the 0+ state at 7.65 Mev in C^{12} is not strongly excited by high-energy protons, but that the next state, at 9.61 Mev, may be so excited. Since the energy of this level is roughly twice that of the first excited state, it is almost correct to assume that inelastic scattering involving the higher level leads to a downward shift by two channels. This fact is not essential to the analysis, but will be used to simplify an illustrative discussion.

Let ϕ_i be the incident flux in the ith channel, and let $Y_L{}^i$ and $Y_R{}^i$ be the scattered yields observed to left and right, respectively, in the ith counter, normalized with respect to ϕ_i. Thus, if the actual scattered fluxes are L_i and R_i, we have for example

$$Y_L{}^i = L_i/\phi_i = (A_L{}^0\phi_i + A_L{}^1\phi_{i+1} + A_L{}^2\phi_{i+2} + \cdots)/\phi_i, \quad (1)$$

with a similar expression for $Y_R{}^i$, where $A_L{}^n$ and $A_R{}^n$ are coefficients, combining the effects of target thickness, differential cross section, and solid angle, relating incident flux to left and right scattering in which the nth state is excited. The asymmetry corresponding to

TABLE I. Illustrative data on elastic separation.

Channel	1	1–2	2	2–3	3	3–4	4	4–5	5
$\phi\times10^{-3}$	850	450	400	300	100	88	12	11	1
x	0.47	0.67	0.25	0.29	0.12	0.13	0.08	0.09	
L	4200	2840	1360	1095	265	236	29	27	2
R	5350	3890	1460	1235	225	203	22	21	1
$Y_L\times10^3$	4.94	6.31	3.40	3.65	2.65	2.68	2.42	2.46	
$Y_R\times10^3$	6.29	8.64	3.65	4.12	2.25	2.31	1.83	1.91	
ϵ	−0.12	−0.16	−0.04	−0.06	0.08	0.07	0.14	0.13	

[11] K. Strauch (private communication).

the nth state alone is therefore

$$\epsilon_n=(A_L{}^n-A_R{}^n)/(A_L{}^n+A_R{}^n), \qquad (2)$$

and we are particularly interested in deducing ϵ_0, the asymmetry in purely elastic scattering. The terms omitted in Eq. (1) are, of course, not simple unless all levels are equally spaced; if the incident spectrum falls off steeply enough, however, such terms rapidly become negligible. The second line of Table I typifies the relative channel fluxes with which we worked in the present measurements. We note now that if we define $x_i=\phi_{i+1}/\phi_i$, and if the third and subsequent terms of Eq. (1) are small, a plot of measured Y_L *vs* x will give a straight line whose slope is $A_L{}^1$ and whose intercept is $A_L{}^0$. To illustrate the procedure, we have chosen coefficients typical of large-angle scattering, where inelastic scattering can predominate. The coefficients are

$$A_L{}^0=2\times10^{-3}, \quad A_L{}^1=5\times10^{-3}, \quad A_L{}^2=5\times10^{-3},$$
$$A_R{}^0=1\times10^{-3}, \quad A_R{}^1=10\times10^{-3}, \quad A_R{}^2=5\times10^{-3},$$

and they imply that

$$\epsilon_0=+0.33, \quad \epsilon_1=-0.33, \quad \epsilon_2=0.$$

The left and right yields that would be observed under these conditions are given in lines 4 and 5 of Table I where, for example, L_1 is given by the sum $1700+2000+500$. Plots of Y_L and Y_R *vs* x are shown in Fig. 2, where the effects of the second excited state are seen as deviations from the dashed straight lines. If the spacing of states were not uniform, the extrapolations would still give $A_{L,R}{}^0$ correctly.

The procedure outlined above leads to the evaluation of left and right elastic cross sections. An alternative extrapolation can be used to give the elastic asymmetry directly. In the notation of Eqs. (1) and (2), the observed asymmetry in the ith channel can be written

$$\epsilon_i=(\epsilon_0+C\epsilon_1 x_i)/(1+Cx_i) \qquad (3)$$

for the case in which only the ground and first excited state are involved in the scattering; here

$$C=(A_L{}^1+A_R{}^1)/(A_L{}^0+A_R{}^0)$$

is the ratio of unpolarized cross sections for inelastic and elastic scattering. If an estimate of this ratio is available from plots of the type described above, one can then examine the intercept and slope of $(1+Cx_i)\epsilon_i$ *vs* x_i for direct evaluation of ϵ_0 and an estimate of ϵ_1. Such a plot, based on the example discussed previously, is shown in Fig. 2, where the effect of the higher state appears to be smaller than in the first method. For situations like the one assumed here, therefore, the second method seems to be preferable for the extrapolation of asymmetries.

B. Alignment

Since one generally finds an extremely rapid variation of differential cross section with angle of scattering,

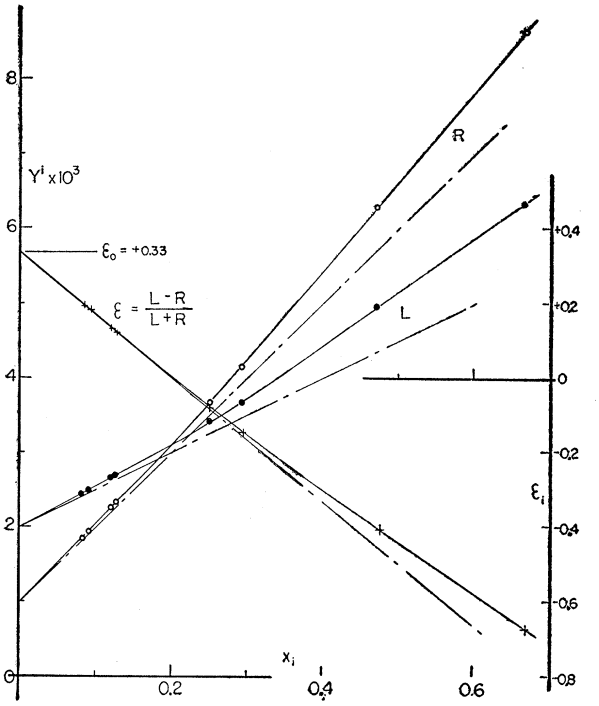

FIG. 2. Left and right second-scattered yields and asymmetries in illustrative example (see text) for which there is strong inelastic scattering involving two excited states of the second scatterer. The dashed straight lines indicate the effect of the first excited state alone. In corresponding experimental data, of course, only the channel differences are statistically independent; the remaining points are plotted here for completeness.

it is important to align the system so that the left and right telescope positions have highly precise *a priori* symmetry about the beam incident on the second scatterer. It is also advantageous to develop methods for confirming geometrical symmetry in the course of the measurements. In our procedure, we began by erecting an accurate transit on a line bisecting the two collimating slits (Fig. 1). The center of the second scatterer, and the vertical axis of the rotating telescope mount, were brought into close coincidence with the line of sight. The angular limits of acceptance in the detecting telescope are fixed in our experiment by the edges of the first two scintillators, and the angle of scattering is read from the line of sight to the line passing through the center of rotation and the centers of these counters. In our measurements, we believe that we knew the angle to an accuracy of two minutes of arc; except at the smallest scattering angles, this uncertainty makes a negligible contribution to the asymmetries observed.

There is another source of misalignment that can be much more serious than the geometrical uncertainty. It arises from the possibility that the collimating slits are not symmetrically irradiated by the polarized beam, so that the mean ray is not coincident with the line of sight established in the manner described. The problem

TABLE II. Study of beam alignment; $\theta=9°$.

Chan.	Slit	Screen	ϵ	Slit	Screen	ϵ	$\Delta\theta$
1–2	2 in.	none	0.630±0.010	8 in.	0.022 in.	0.606±0.008	−0.25±0.10 deg
2–3			0.613±0.008			0.594±0.009	−0.15±0.10
3–4			0.513±0.012			0.540±0.013	+0.35±0.13
4			0.42 ±0.03			0.46 ±0.06	+1.1 ±0.6
1–2	2 in.	0.124 in.	0.57 ±0.01	8 in.	0.124 in.	0.580±0.006	0.00±0.10
2–3			0.58 ±0.01			0.585±0.008	−0.05±0.10
3–4			0.56 ±0.01			0.563±0.012	+0.15±0.13
4			0.62 ±0.03			0.48 ±0.03	+0.9 ±0.3

has been handled through a series of measurements and assumptions that will now be outlined. First, profiles of the beam intensity were measured across the exit face of the steering magnet. Energies were chosen at several points in the high-energy tail of the spectrum. It was found that, for all energies, the distribution is quite flat over several inches at the center of the magnet face. The first slit width was set at two inches, and a study made of asymmetries measured in four channels at the scattering angle 9°. The angle is small enough so that one can assume elastic scattering to predominate. According to Eq. (3), one then expects ϵ_i to be independent of x_i and equal to ϵ_0 for all channels. We are further assuming, of course, that the elastic polarization is independent of energy over an interval of about 13 Mev. In a later discussion (Sec. III) it will be indicated that such a flatness exists.

When asymmetries were measured under these conditions, they were found to decrease with increasing energy. The first entries of Table II are typical of the results. The trend here is consistent with the assumption that the illumination of the second slit is not uniform for all channels, and that incident protons in the highest channels are weighted toward the right side of the slit, as one would expect. In order to smooth out the illumination, we introduced a 0.124-inch copper screen at the exit face of the steering magnet, and restored the channel energies by removing an equal thickness of absorber from the detecting telescope. The data of Table II indicate that this modification brought the asymmetries into fair agreement. We now make the principal assumption of this procedure, which is that the asymmetries tend to converge to the true value. The assumption is based on our confidence in the geometrical symmetry of the left and right telescope positions, and in the freedom of the measurements from other sources of angular error.

In order to obtain adequate counting rates in measurements at large scattering angles, it was necessary to increase the width of the first slit and to reduce the thickness of the copper screen. We found that each of these steps introduced new angular errors; we therefore calibrated the effective angular error of each channel by measuring the sensitivity of the corresponding asymmetry to small rotation of the reference line, and then deducing the angular shift that would bring the asymmetry to the true value. The results appear as the remaining data in Table II; under $\Delta\theta$ are given the effective angular errors so deduced. We point out that unsymmetrical illumination of the wide first slit, which apparently introduces most of the error, leads to a correction that is independent of angle of second scattering. It can furthermore be shown that, with the second target geometry used here, the correction arising from poor illumination of the second slit has no significant dependence on angle. We therefore based the corrections at all angles on the $\Delta\theta$ values of Table II. The low counting rate and relatively large $\Delta\theta$ in channel 4 discouraged us from using it in deducing yields and asymmetries. It was needed, however, for estimating ϕ_4 and x_3.

Finally, we wish to note here that the assumption of pure elastic scattering in the small-angle region has been fairly well confirmed by a set of direct measurements of proton spectra. It was found, for example, that the pulse-height spectrum of the incident beam is indistinguishable from the spectrum of protons scattered through 15° from C^{12}. The sensitivity of the measurement was checked by observing the broadening of the incident spectrum with half of the beam reduced in energy by 4.4 Mev. The results imply that we could have seen a 10% contamination of inelastic scattering involving the first excited state, and correspondingly less for the higher states.

C. Second Target and Detector

For the extrapolation procedures to be strictly valid, it is necessary that the shape of the spectrum of elastically scattered protons be independent of scattering angle. Aside from very small effects due to variation of straggling and nuclear recoil,[12] this condition can be accurately achieved by orienting a flat target so that, for scattering angle θ, the target normal is at $\theta/2$. A mechanism for accomplishing this automatically has been built into the target assembly. The graphite target used for most of the measurements had a thickness of 4.0 g/cm², with energy losses that were almost completely independent of the depth at which scattering occurred.

At $\theta=4°$, the smallest angle at which measurements have been taken, the contribution to the yield of

[12] We do not mean to imply here that we have ignored the *average* recoil losses, which were in fact compensated for by adjustment of the absorbers.

multiple Coulomb scattering is expected to be small. Calculation of $\langle\theta\rangle$ for multiple scattering in our target gives 0.9°. An experimental check on the effect was made by repeating the small-angle measurements with a target of thickness 1.0 g/cm². No change in the asymmetries was found. There is another small-angle effect arising from the fact that a fixed counter geometry spans a larger interval in azimuth at small angles than at large angles. We found that this effect is small for all $\theta > 6°$; we reduced beam and counter heights in taking final data below 10° so as to be certain that no correction would be necessary.

The target and detector geometry, oriented for scattering to the left, can be seen in Fig. 3. The compensating absorber has the same stopping power as the target, and is automatically inserted when the target is retracted for background measurement. Counters A and B define the scattered beam and, when they have the dimensions shown in Fig. 3, give a triangular resolution function with a base of width 6°. The main absorber thickness is chosen to give channel flux ratios approximating those of Table I. As θ is increased, the main absorber thickness is decreased to make up for increasing ionization and recoil losses in the target, and so to maintain constant channel energies. The first recorded coincidence is derived from signals in A, B, and 1. Subsequent coincidences are made by adding the next signal to the coincident output of all previous counters.

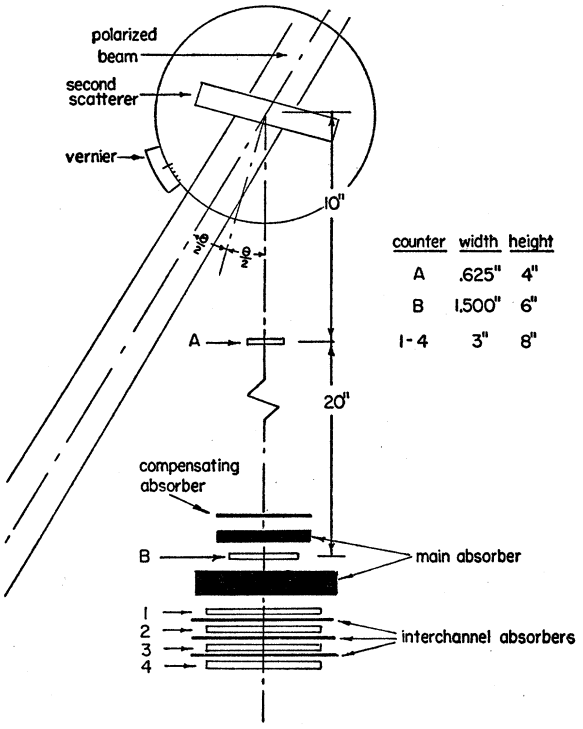

FIG. 3. Detail of second scatterer and counter telescope, set for scattering through an angle θ to the left. The widths of counter B and the second slit were reduced for measurements below 13°, giving the improvement in angular resolution shown.

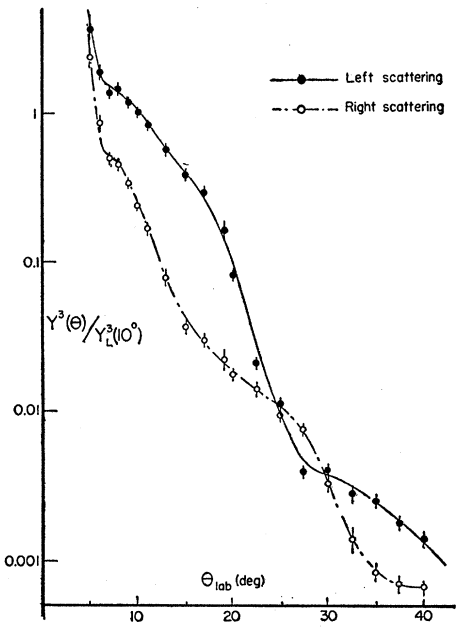

FIG. 4. Relative left and right yields observed in channel 3 after second scattering. These are raw data corrected only for angular error (see text).

It is insured that all of the four final counters have identical energy-loss thresholds. There are no difficulties with accidental coincidences or counting losses.

III. RESULTS

The data from these measurements took the form of counting rates to left and right of the polarized beam, normalized to the incident flux, and recorded in four statistically independent energy channels. For scattering angles above 20°, where a wide first slit was used, the data require correction for angular error, as discussed in the previous section. An additional correction to the raw data is needed as a result of the fact that the differential cross sections are energy dependent, whereas we wish to examine the data from all channels after normalization to the same incident energy. The corrections are straightforward and need not be discussed further. The corrected left and right differential cross sections as observed in channel 3 (the highest channel in which the counting rate was usable) are given in Fig. 4, and the corrected asymmetries observed in three successive channels are shown in Fig. 5. We note that the cross sections do not exhibit very strong diffraction effects, and that the asymmetries for scattering angles above 20° are critically dependent upon channel number. We interpret these features of the data as consequences of admixtures of inelastic scattering. An obvious clue to such an interpretation comes from the observation that the asymmetries in channel 3, which is expected to contain the least inelastic admixture, are the closest in their behavior to predictions from the optical model. The following discussion will

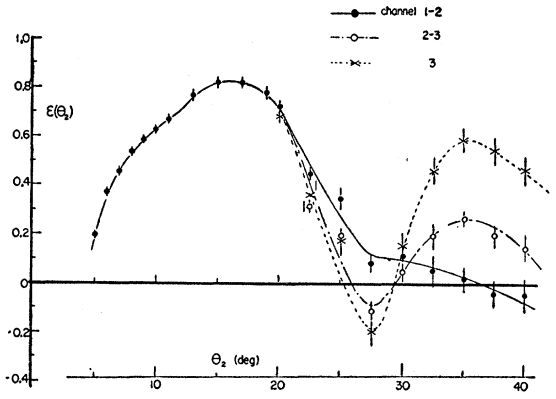

FIG. 5. Asymmetries observed in three statistically independent channels spaced 4.4 Mev apart. Channel 3 accepts protons of the highest energy. The data are corrected for angular error, and the abscissas are adjusted to correspond to a fixed incident energy of 220 Mev.

summarize the attempts that have been made in extrapolating the data to pure elastic scattering.

In order to apply the extrapolation techniques of Sec. IIA, we must deduce values for the abscissas x_i, defined as the ratio of incident fluxes in a pair of adjacent channels. At sufficiently small scattering angles, x_i is equally well given by ratio of scattered fluxes, since the shape of the incident spectrum is preserved in the absence of significant amounts of inelastic scattering. We therefore took the values from scattering data at 10°. Figure 6 shows typical extrapolations of left and right scattering at three scattering angles: at 20° the asymmetry is positive and the inelastic contribution is still small; at 27.5° the elastic asymmetry is negative and the inelastic asymmetry is positive; at 40° the elastic asymmetry has passed through a second positive maximum and the inelastic asymmetry has become negative. The relative elastic and inelastic cross sections, taken from the intercepts and slopes of such plots, are shown in Figs. 7 and 8. We see that the separation procedure

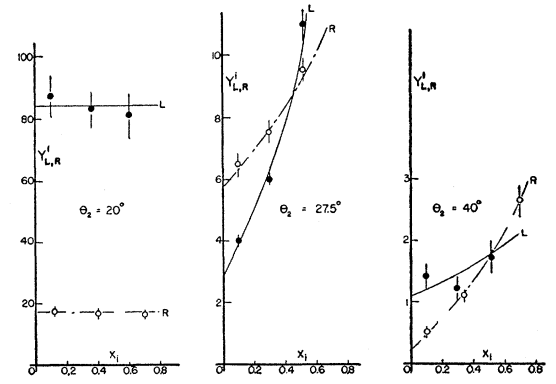

FIG. 6. Typical left and right extrapolated channel yields obtained in this experiment. The vertical scales are arbitrary. The intercepts of these plots give yields for purely elastic scattering; initial slopes give estimates of inelastic yields for scattering that leaves C^{12} in its first excited state. See text for notation and further discussion.

reveals a fairly strong diffraction minimum near 30° in elastic scattering to the left, and that in this region the inelastic competition is very much stronger, perhaps by a factor of ten or more. It is clear that, under such conditions, a small admixture of inelastic scattering can easily fill in a diffraction minimum, and that the present methods are probably not adequate for accurate exploration of these regions.

Having estimated separately the elastic and inelastic asymmetries by the methods described, we wish next to convert them to the corresponding polarization functions. It is well known[13] that, for the special case of elastic scattering of nucleons by spinless nuclei, the relation

$$\epsilon(\theta_2)=P_1(\theta_1)P_2(\theta_2) \tag{4}$$

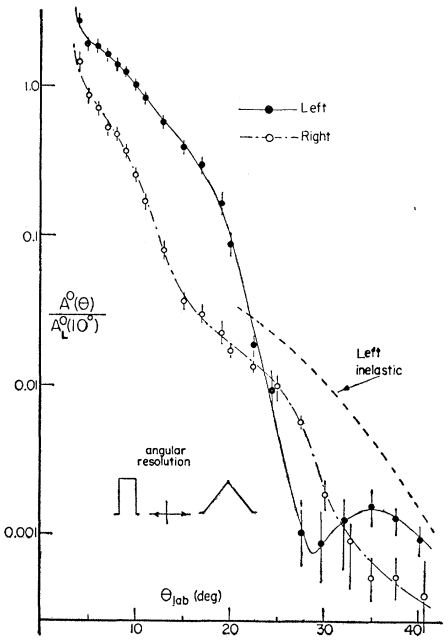

FIG. 7. Extrapolated left and right elastic yields, relative to the leftward count at 10 degrees. Note the stronger evidence than is seen in Fig. 4 for a diffraction minimum at 29 degrees. The estimated leftward yield of inelastic scattering (Fig. 8) is superimposed for comparison.

holds for a double scattering, where $\epsilon(\theta_2)$ is the asymmetry of second scattering, $P_1(\theta_1)$ is the polarization produced in first scattering, and $P_2(\theta_2)$ is the polarization that would be produced in second scattering if the incident beam were unpolarized. No analogous theorem has yet been established for inelastic scattering. The magnitude of P_1 can therefore be calibrated only if an asymmetry is measured under conditions guaranteeing that both scatterings are elastic, and that the energies and angles of both scatterings are identical. In our experiment, θ_1 was determined by orbit computation to be 14.0° with an uncertainty of about one degree. As a result of material in the beam between the two

[13] L. Wolfenstein and J. Ashkin, Phys. Rev. **85**, 947 (1952).

targets, the energy at second scattering was reduced to about 220 Mev from a primary energy of 240 Mev. From the fact that, for constant strength of potential in Born approximation, $P(k,R,\theta)$ is constant when

$$kR\sin\theta/2=\text{const},\tag{5}$$

we expect that the second scattering angle 14.7° is equivalent to the first angle 14.0°. The question of pure elasticity in the second scattering was discussed in Sec. IIB; we can also see from the results of extrapolation (Figs. 7 and 8) that inelastic scattering cross sections are relatively very small below 20°. The same conclusion, of course, applies to the first scattering as well. We are therefore confident that Eq. (4) is valid for the calibration, and from the measured asymmetry at 14.7° we deduce for the primary polarization

$$P_1(14.0°)=+0.89\pm0.02,\tag{6}$$

where the experimental error includes counting statistics, uncertainty in θ_1, and uncertainty in telescope alignment. It has been assumed that the strength of the polarization, at its maximum, is independent of energy in the region around 220 Mev. There is in fact a flat maximum at this energy, according to data recently reported.[14] With the value of P_1 given by Eq. (6), we have used Eq. (4) to convert elastic and inelastic second-scattering asymmetries, extrapolated by the methods of Sec. II, into the functions $P(\theta)$ shown in Fig. 9. The function represents the true polarization for the elastic scattering, but the status of the curve for inelastic scattering must remain ambiguous until Eq. (4) has been confirmed or corrected for this case. The sign of the polarization adopted in Eq. (6), which implies that a scattering to the left at this angle induces a predominance of upward spin, is not given by this experiment, but is taken as a consequence of choosing the sign of $L\cdot S$ coupling to be the same as in shell theory.

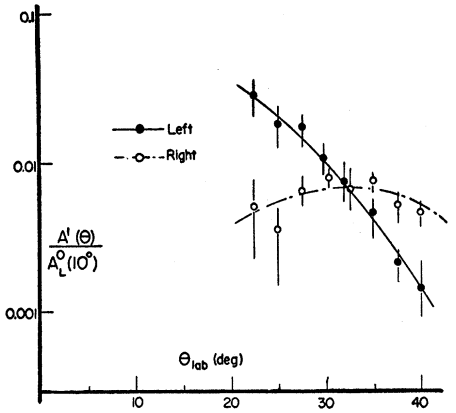

FIG. 8. Estimates, based on plots of the type shown in Fig. 6, of left and right inelastic yields, relative to the leftward elastic yield at 10 degrees. Inelastic scattering is found to predominate at scattering angles above 25 degrees.

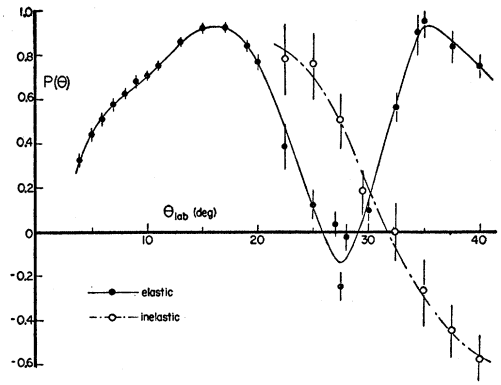

FIG. 9. The solid curve is the angular dependence of polarization in elastic scattering of protons by C^{12} at 220 Mev, obtained by extrapolation methods discussed in the text. The dashed curve is an estimate of polarization in inelastic scattering, computed on the assumption that Eq. (4) holds for this process. Below 22 degrees, the admixture of inelastic scattering is too small for these estimates to be made.

One can readily see that the elastic polarization obtained for C^{12} is in good qualitative agreement with predictions[15] from the optical model. Perhaps the most interesting feature of the result is the appearance of a very strong second maximum in $P(\theta)$ at 35°. Such a peak appears consistently in most calculations of which we are aware.[4–7,15–17] The other significant features of the elastic polarization are the indication of Coulomb interference at 10° and below, which is an effect also observed in the Harwell measurements[18]; the sharp minimum, going to slightly negative polarization, at 27.5°; and the very high polarization in the first maximum. The failure of the minimum and second maximum to appear in the Berkeley measurements[19] is probably attributable to inelastic admixture in the scattered beam, since our results in channel 1–2 (Fig. 5), which contain significant amounts of inelastic scattering, appear very similar to the C^{12} results reported from Berkeley. We also wish to note that the Berkeley measurements[19] on He^4, in which there can be no question of inelastic contamination, need not be in disagreement with predictions of the optical model. In fact, using Eq. (5) to correct for change in wave number and nuclear radius, we find on the basis of the present data that the first minimum in He^4 would occur at a laboratory angle of 33° for an incident energy of 316 Mev. The speculation is not inconsistent with the Berkeley data in this angular region.

We have begun measurements on the elastic polariza-

[14] K. Strauch, University of California Radiation Laboratory UCRL-3211, November, 1955 (unpublished).

[15] R. M. Sternheimer, Phys. Rev. **97**, 1314 (1955).
[16] Fernbach, Heckrotte, and Lepore, Phys. Rev. **97**, 1059 (1955).
[17] R. M. Sternheimer, Phys. Rev. **100**, 886 (1955).
[18] Dickson, Rose, and Salter, *Proceedings of the Fifth Annual Rochester Conference on High-Energy Physics* (Interscience Publishers, Inc., New York, 1955).
[19] Chamberlain, Segrè, Tripp, Wiegand, and Ypsilantis, Phys. Rev. **96**, 807 (1954).

tion in heavier nuclei. Preliminary results for the case of Ca^{40} show a striking resemblance to the data of Fig. 9, after adjustment of abscissas on the basis of Eq. (5). It is found, in agreement with other observations,[20,21] that the polarization minimum corresponding to the dip in C^{12} at 27.5° is not completely washed out in the low energy channels, implying that inelastic scattering is competing less strongly in the heavier nucleus. This may simply be a result of the fact that the diffraction pattern is moving into smaller angles, together with the possibility that inelastic scattering is much less dependent on nuclear radius. In any event, we suspect that previously reported strong variations of the large-angle behavior with nuclear mass can be explained by differences in inelastic contributions.

[20] T. Ypsilantis and R. Tripp (private communication).
[21] Chamberlain, Segrè, Tripp, Wiegand, and Ypsilantis, Phys. Rev. **95**, 1105 (1954).

ACKNOWLEDGMENTS

The authors wish to acknowledge the assistance of Professor J. Tinlot and E. Baskir, R. Harding, and S. Spital. We wish also to thank the cyclotron crew of the 130-inch laboratory for their excellent cooperation.

PHYSICAL REVIEW VOLUME 104, NUMBER 2 OCTOBER 15, 1956

Energy Levels of Be^9†

C. K. BOCKELMAN,* A. LEVEQUE,‡ AND W. W. BUECHNER
Laboratory for Nuclear Science and Department of Physics, Massachusetts Institute of Technology, Cambridge, Massachusetts
(Received July 2, 1956)

Magnetic analysis of the alpha-particle groups from the deuteron bombardment of boron and of the proton groups from the proton bombardment of beryllium confirms previous work indicating the existence of levels in Be^9 at 2.43 and 3.04 Mev. The energy of the edge of a broad distribution at 1.664-Mev excitation is taken to indicate that it arises from a three-body reaction; the shape of the edge indicates the influence of the Be^8—n interaction.

I. INTRODUCTION

THE energy levels of the Be^9 nucleus have been the subject of several recent studies.[1–3] These experiments have been concerned with verifying the results of Moak *et al.*[4] and Almqvist *et al.*,[5] which showed that the $Li^7(He^3,p)Be^9$ and the $B^{10}(t,\alpha)Be^9$ reactions displayed a characteristic edge to the proton and alpha distributions which was interpreted as evidence for a state at 1.8 Mev in Be^9. In addition, the well-known level at 2.428 Mev[6–8] as well as a broad group attributed to a 3.1-Mev state were observed. Lee and Inglis[1] saw alpha groups from the deuteron bombardment of boron which they assigned to Be^9 levels at 1.75 Mev, 2.43 Mev, and 3.02 Mev. However, Gosset *et al.*[2] in a study of the inelastic protons from a Be^9 target carefully measured the edge of a proton distribution, which corresponded to an excitation of 1.675±0.002 Mev. They suggested that these protons, rather than signifying a 1.8-Mev level in Be^9, might be associated with the (p,pn) reaction, since the edge energy corresponded closely to the (γ,n) threshold in Be^9 measured as 1.666±0.002 Mev by the Wisconsin group[9] and as 1.662±0.003 Mev at Notre Dame.[10] The small difference between the edge and the threshold was attributed to a barrier effect. Finally, Rasmussen *et al.*,[3] studying the inelastic scattering of deuterons and alphas from Be^9, again saw a broad distribution with a maximum in the neighborhood of 1.74-Mev excitation, the sharp state at 2.43 Mev, and the broad state at 3.1 Mev. By analyzing the shape of the distribution, these authors attempted to answer the question of whether the 1.74-Mev maximum is a state or the edge of a continuum from the three-body breakup. The present work was undertaken concurrently with the work described in references 2 and 3. It was felt that the use of the broad-range spectrograph,[11] which permits the simultaneous recording of a wide energy range of reaction products,

† This work has been supported in part by the joint program of the Office of Naval Research and the U. S. Atomic Energy Commission.
* Now at Yale University, New Haven, Connecticut.
‡ Permanent address: Centre d'Etudes Nucléaires de Saclay, France.
[1] L. L. Lee, Jr., and D. R. Inglis, Phys. Rev. **99**, 96 (1955).
[2] Gossett, Phillips, Schiffer, and Windham, Phys. Rev. **100**, 203 (1955).
[3] Rasmussen, Sampson, Miller, and Gupta, Phys. Rev. **100**, 851 (1951).
[4] Moak, Good, and Kunz, Phys. Rev. **96**, 1363 (1954).
[5] Almqvist, Allen, and Bigham, Phys. Rev. **99**, 631(A) (1955).
[6] Van Patter, Sperduto, Huang, Strait, and Buechner, Phys. Rev. **81**, 233 (1951).
[7] Browne, Williamson, Craig, and Donahue, Phys. Rev. **83**, 179 (1951).
[8] Arthur, Allen, Bender, Hausman, and McDole, Phys. Rev. **88**, 1291 (1952).
[9] R. C. Mobley and R. A. Laubenstein, Phys. Rev. **80**, 309 (1950).
[10] Noyes, Van Hoomisen, Miller, and Waldman, Phys. Rev. **95**, 396 (1954).
[11] Beuchner, Mazari, and Sperduto, Phys. Rev. **101**, 188 (1956).